Cancer Research

# FLT-PET Is Superior to FDG-PET for Very Early Response Prediction in NPM-ALK-Positive Lymphoma Treated with Targeted Therapy

Zhoulei Li, Nicolas A Graf, Ken Herrmann, et al.

*Cancer Res* Published OnlineFirst August 8, 2012.

**RESEARCH ARTICLE**

# FLT-PET Is Superior to FDG-PET for Very Early Response Prediction in NPM-ALK-Positive Lymphoma Treated with Targeted Therapy

Zhoulei Li[1]*, Nicolas Graf[2]*, Ken Herrmann[1], Alexandra Jünger[1], Michaela Aichler[3], Annette Feuchtinger[3], Anja Baumgart[2], Axel Walch[3], Christian Peschel[2], Markus Schwaiger[1], Andreas Buck[4], Ulrich Keller[2#], and Tobias Dechow[2,5#]

[1] Nuclear Medicine, Technische Universität München; Munich, Germany

[2] III. Medical Department, Technische Universität München; Munich, Germany

[3] Pathology, Helmholtz Zentrum München; Munich, Germany

[4] Nuclear Medicine, Universitätsklinik Würzburg; Würzburg, Germany

[5] Onkologie Ravensburg, Ravensburg, Germany

[*,#] contributed equally

**Corresponding Author:**

Tobias Dechow, MD
III. Medical Department
Technische Universität München
Ismaningerstr. 22
D-81675 Munich
Germany
Phone: +49 751 366197 0
Fax: +49 751 366197 66
E-mail: t.dechow@lrz.tum.de

**Running title:** FLT-PET for early response prediction in ALCL

**Key words:** Functional Imaging; FLT-PET; FDG-PET; Lymphoma; NPM-ALK; Targeted Therapy

**Abstract:** 250 words

**Total word count:** 5553 words

**Conflicts of Interest:** None.

## Abstract

The prognosis of relapsed or refractory aggressive lymphoma is poor. The huge variety of currently evolving targeted treatment approaches would benefit from tools for early prediction of response or resistance. We used various ALK-positive anaplastic large cell lymphoma (ALCL) cell lines to evaluate two inhibitors, the HSP90 inhibitor NVP-AUY922, and the mTOR inhibitor everolimus, both of which have shown to interfere with ALK-dependent oncogenic signal transduction. Their therapeutic effect was determined *in vitro* by MTT assay, [$^{18}$F]fluorodeoxyglucose- (FDG) and [$^{18}$F]fluorothymidine- (FLT) uptake, and by biochemical analysis of ALK-induced signalling. Micro FDG- and FLT-PET imaging studies in immunodeficient mice bearing ALCL xenotransplants were performed with the cell lines SUDHL-1 and Karpas299 to assess early treatment response to NVP-AUY922 or everolimus *in vivo*. SUDHL-1 cells showed sensitivity to both inhibitors *in vitro*. Importantly, we detected a significant reduction of FLT-uptake in SUDHL-1 bearing animals using both inhibitors compared to baseline as early as 5 days after initiation of targeted therapy. Immunostaining showed a decrease in Ki-67 and an increase in cleaved caspase-3 staining. In contrast, FDG-uptake did not significantly decrease at early time points. Karpas299 xenotransplants, which are resistant to NVP-AUY922 and sensitive to everolimus treatment, showed an increase of mean FLT-uptake on day 2 after administration of NVP-AUY299, but a significant reduction in FLT-uptake upon everolimus treatment. In conclusion, we show that FLT- but not FDG-PET is able to predict response to treatment with specific inhibitors very early in the course of treatment and thus enables early prediction of treatment efficacy.

## Introduction

The standard therapy for aggressive Non-Hodgkin lymphoma (NHL) are CHOP-like regimes, in the case of B cell origin combined with Rituximab (1). However, not all aggressive NHL patients show a favourable outcome. Relapsed or refractory disease is a substantial clinical problem with a poor prognosis. Based on molecular insights into different lymphoma subtypes, a large number of druggable molecules have been identified. These molecules include receptor signalling molecules (e.g. BTK, Syk, PKCβ), anti-apoptotic proteins, deacetylases, and immune modulators (2, 3). Although these approaches are promising a substantial number of patients does not benefit from these targeted therapeutics. Given that various novel compounds will be available for the treatment of relapsed/refractory lymphoma in the future, the implication of predictive biomarkers will be critical. However, regression of lymphomas in the course of the therapy is a very important endpoint. Thus, evaluation of response early in the course of the therapy will help to optimize treatment modalities, avoid ineffective treatment, and reduce costs.

FDG-PET imaging has been successfully used for imaging lymphoma with proven implications for prognosis after completion of therapy (4, 5). In addition, interim FDG-PET has been used to monitor response to therapy (6, 7). In these studies interim PET was predictive for progression-free and overall survival (PFS, OS). However, in some studies the specificity and predictive value of interim PET was very limited (8, 9). In a study that included biopsies of PET-positive lesions, FDG-PET was not predictive for PFS (10). These limitations are based on the fact, that FDG uptake is not tumor-specific and false-positive findings can be generated by inflammation (11). Tracers that are capable to distinguish lymphoma tissue from inflammatory tissue are required.

Deregulated cell cycle progression is a hallmark of cancer. With respect to *in vivo* imaging, proliferative activity has been shown to be more specific for malignant tumors than that of glucose metabolism (12). The thymidine analogue 3′-deoxy-3′-[$^{18}$F]fluorothymidine (FLT) is a stable PET tracer that accumulates in proliferating tissues and malignant tumors (13). In line, the thymidine kinase 1 has been revealed as a key enzyme responsible for the intracellular trapping of FLT (14). Several studies in humans showed a significant correlation of tumor proliferation and FLT uptake (15-17). As a preclinical model for monitoring therapeutic response, a significant decrease of FLT uptake was observed in tumor-bearing mice as early as 24hr after chemotherapy (18-20). We showed that the reduction of FLT

uptake in aggressive lymphomas after the first course of therapy correlates with response at the end of the treatment (21).

50-60% of anaplastic large cell lymphoma (ALCL) are associated with the t(2;5)(p23;q53) chromosomal translocation involving the anaplastic lymphoma kinase (ALK) gene (22, 23). The t(2;5) results in the expression of the oncogenic fusion protein nucleophosmin-anaplastic lymphoma kinase (NPM-ALK). A number of studies have shown that the constitutively active tyrosine kinase function of NPM-ALK is a key oncogenic event in the pathogenesis of t(2;5)-positive ALCLs, which leads to the constitutive activation of several signaling pathways including the STAT3, PI-3K/Akt and mTOR pathways (24, 25). Thus, ALK as well as ALK-dependent signalling events constitute therapeutic targets for the treatment of ALCL. Besides ALK inhibitors, which are now being tested in preclinical and clinical studies, heat shock protein 90 (HSP90) inhibition leading to ALK degradation as well as mTOR inhibition are highly effective approaches to ALK-positive ALCL cells *in vitro* (26, 27).

In this report, severe combined immunodeficient (SCID) mice bearing ALK-positive lymphoma xenotransplants were treated with the HSP90 inhibitor NVP-AUY922 (AUY922) and the mTOR inhibitor everolimus. Micro PET imaging using FDG and FLT as tracer was applied to predict response to targeted therapy very early in the course of treatment. Our studies contribute to the understanding of functional imaging in lymphoma exposed to pathway-specific drugs and provide the opportunity to individualized targeted treatment.

## Materials and Methods

### Cell lines and animals

The human t(2;5) ALCL cell lines SUDHL-1, Karpas299, and SR-786 were obtained from and propagated as suggested by the German Collection of Microorganisms and Cell Cultures (DSMZ) and were authenticated by DSMZ using DNA-typing and PCR analysis as well as cytogenetic testing. Cells used for all experiments were passaged for fewer than 6 months after receipt. JB-6 were obtained from S. Morris (Memphis, USA). Ba/F3 cells (originally obtained from DSMZ) transfected with NPM-ALK (Ba/F3-NA) were obtained from Justus Duyster (Munich, Germany). Cells were cultured in RPMI 1640 medium containing 10% fetal bovine serum, 1mM L-glutamine and 1% penicilline/streptomycine (Gibco). 6-8 week old female immunodeficient mice (CB-17 SCID) were obtained from Charles River Laboratories.

For induction of tumors $10\times10^6$ SUDHL-1 or $5\times10^6$ Karpas299 cells suspended in sterile PBS (100µl) were injected subcutaneously into the right shoulder region. All animal experiments were authorized by the regional government agency (Regierung von Oberbayern, Az. 55.2-1-54-2531-52-07).

## Inhibitors

AUY922 (HSP90 inhibitor) and everolimus (mTOR inhibitor) were provided by Novartis. AUY922 and everolimus were solubilized in 5% glucose to 200µM or 1µM stock solution and stored at -20°C. The primary solution was diluted to 0-1000nM for AUY922 and 0-100nM for everolimus with RPMI 1640 medium for cell culture.

## MTT assay

MTT assays were performed according to the manufacturer's instruction (Promega). Briefly, $10^4$ SUDHL-1 or Karpas299 cells per well (96-well plate) were incubated at 37°C with different concentration of inhibitors for 48hr. 20µl of MTT dilution (3-(4,5-dimethylthiazol-2-yl)-2,5-diphenyltetrazoliumbromide in PBS) was added per well and cells were incubated for 90min. Absorbance was measured at 570nm using a Bio-Tek ELx800™ Series Universal Microplate Reader (Progen Scientific).

## Flow cytometry

Lymphoma cells ($5x10^5$/well in 12-well plates) were incubated with inhibitors at 37°C. After 48hr cells were centrifuged (1700U/min, 7min) and stored in 3ml ethanol (70%) at -20°C. On the day of analysis, cells were centrifuged again and resuspended in 300µl PBS. After RNA-digestion by ribonuclease A (Sigma-Aldrich 95%), propidium iodine (Sigma-Aldrich) was added in a 1:500 dilution. Cells were incubated for 30min at 37°C and analyzed (Beckman Coulter). To assess apoptosis, $5x10^5$ cells were stained with FITC-labeled AnnexinV (BD Pharmingen) and counterstained with propidium iodide (Sigma-Aldrich). Following incubation cells were washed, resuspended in PBS, and analyzed by flow cytometry (Beckman Coulter).

## Immunoblotting

Cells were incubated with inhibitors at 37°C. After 48hr cells were washed, pelleted and stored at -80°C. Cells were lysed and the protein concentration was determined using protein assay dye reagent (Bio-Rad) with bovine serum albumin as standard. For immunoblotting

50µg protein per lane was separated on a 7.5% gradient readymade SDS-Gel (BioRad) and transferred to a PVDF (Millipor Corporation) membrane. Primary antibodies (ALK or p-Tyrosine-ALK, AKT or p-AKT, STAT3 or p-STAT3, p70S6K or p-p70S6K, all from Cell Signaling) were diluted to 1:200 into blocking buffer and incubated over night at 4°C, washed, and incubated with secondary antibody. Blots were developed using Pierce Fast Western Blot Kit and exposed to film (Fisher Themo Scientific).

### FLT- and FDG-uptake *in vitro*

Lymphoma cells ($5\times10^5$/ well in 12-well plates) were incubated with different concentrations of inhibitors at 37°C for 48hr. After cell counting, 100µl of tracer solution was added and incubated (45min, 37°C). Tracer solution consisted of 0.9% sodium chloride and FLT or FDG with an activity of 370kBq. Cells were washed three times with PBS before measuring activity in counts per minute (cpm) using an automated gamma-counter (Cobra II, Packard Instrument). Results of cells were adjusted to $10^6$ cells per well. The cellular uptake of tracer was calculated utilizing the formula [original cpm of cells/standard value (cpm)]*100%.

### Tumor volume and therapeutic regimens

Tumor diameters were measured daily with a shifting calliper and tumor volume was calculated using the formula [length x $(\text{width})^2$]/2. Treatment was performed when the xenotransplants reached a size of approximately 500mm³. Lymphoma bearing animals were treated daily with AUY922 (25mg/kg i.p.), everolimus (5mg/kg p.o.) or carrier (glucose 5% i.p. or p.o.).

### PET-Imaging

3'-[$^{18}$F]fluoro-3'-deoxythymidine and 2-deoxy-2-[$^{18}$F]fluoro-D-glucose were synthesized as previously described (28) (Radiopharmacy Unit, TU München). Imaging was performed using a micro PET system (Inveon, SIEMENS Preclinical Solutions), FLT or FDG was administered via tail vein injection (100µl) at an activity dose of 5-10MBq per mouse. The accumulation of radiotracer in the tumor was allowed for 60min. Mice were then imaged for a 15min static acquisition.

### PET data analysis

Tumor-to-background ratios (TBR) were calculated to semi-quantitatively assess the tracer accumulation in the tumor. Circular 3D regions of interest (ROIs) were placed manually in the

area with the highest tumor activity. The diameter was not covering the entire tumor volume to avoid partial volume effects. For determination of background activity, two 3D ROIs were placed in the spinal muscle at the level of the kidneys. Corresponding TBR, $mean_{tumor}/mean_{muscle}$ were calculated.

### Histological and immunohistochemical analysis

Formalin-fixed, paraffin-embedded sections (5µm) of resected tumor tissue were dewaxed, rehydrated and microwaved for 30min in a 0.01M citrate buffer, pH 6.0 containing 0.1% Tween 20. Sections were washed in Tris-buffered saline (pH 7.6) containing 5% fetal calf serum (Life Technologies) for 20min. The primary antibodies used were: anti-Ki-67 antigen antibody solution (MIB-1, M7240, Dako; 1:75 diluted with Antibody Diluent (Dako ChemMate), anti-cleaved caspase-3 rabbit antibody solution (Asp175, Cell Signaling). The remainder of the procedure was performed on the automated immunostainer (DISCOVERY XT, Ventana Medical System). Diaminobensidine (Ventana Medical System) liquid served as chromogen.

### Statistical analysis

Statistical analyses were performed using the statistical function of Excel 2007 (Microsoft) or GraphPad Prism 5 (GraphPad Software). A p-value $<0.05$ was considered statistically significant as assessed by t-test.

## Results

### FLT uptake is a sensitive measure for HSP90 inhibition of NPM-ALK+ ALCL *in vitro*

SUDHL-1 ALCL cells depend on the constitutive activity of the ALK kinase that results from the *NPM-ALK* t(2;5)(p23;q53) translocation (23, 29). Complex formation of NPM-ALK with HSP90 is critical to prevent degradation of the oncogene (26). Using MTT assays, SUDHL-1 cells showed sensitivity to a 48hr treatment with the HSP90 inhibitor AUY922 with a maximum effect at the 100nM dose level and an $IC_{50}$ of less than 10nM (Fig. 1A). PI staining revealed that AUY922 induced both cell cycle arrest and cell death as demonstrated by a significant decrease of the S phase fraction and a marked increase of the G0/G1 fraction as well as a higher number of AnnexinV-positive cells (Fig. 1B). In the presence of AUY922,

expression of phosphorylated and total NPM-ALK was dramatically reduced in a dose-dependent manner after 48hr (Fig. 1C). Moreover, the downstream signalling molecules STAT3 and AKT (24) as well as their phosphorylated forms were virtually undetectable at the 50nM dose level. To estimate whether HSP90-NPM-ALK-targeted treatment with AUY922 was assessable by measuring FDG and FLT uptake, we determined the cellular tracer uptake of FLT and FDG in AUY922 treated cells. SUDHL-1 cells were incubated with FLT or FDG for 45min after a 48hr treatment period and the activity was measured using a gamma-counter. HSP90 inhibition led to a significant reduction of both FLT and FDG uptake in SUDHL-1 cells (Fig. 1D). However, sensitivity of FLT was significantly higher showing a complete lack of FLT uptake in the presence of 25nM AUY922. In contrast, FDG uptake was only reduced by 40% compared to the vehicle-treated control at the same dose level. These *in vitro* results were confirmed by the additional analysis of the NPM-ALK positive ALCL cell lines JB-6 and SR-786 and murine B cells expressing ectopic NPM-ALK. Although these cells were sensitive to AUY922 treatment to various extents, early response monitoring revealed superiority of FLT as a tracer over FDG (Supplemental Fig. S1A-C). These data suggest that FLT might be a suitable tracer particularly to determine effective NPM-ALK-targeted treatment *in vitro*.

## Functional *in vivo* imaging of response to HSP90 inhibition in SUDHL-1 lymphoma by FLT-PET is superior to FDG-PET

To evaluate FDG- and FLT-PET imaging for early response monitoring *in vivo*, we generated xenograft SUDHL-1 tumors. To mimic the clinical situation treatment was initiated once tumor volume reached approximately 500mm³. The control group showed a 3-fold (n=4, mean 3.0-fold, SD=1.5, range 2.1-5.6-fold) increase in tumor volume (Fig. 2A). In contrast, tumors of AUY922-treated mice remained nearly constant during the observation period (n=12, mean 1.3-fold increase, SD=0.3, range 0.7-1.7-fold). Notably, extended treatment beyond 14 days resulted in a slight reduction of the tumor volume in three mice (mean 0.8-fold, SD=0.3, range 0.7-1.1-fold) (data not shown). To determine the predictive value of early functional imaging for response assessment we performed FDG- and FLT-PET scans before and five days after initiation of AUY922 treatment. To do so, change of TBR on day 5 compared to pre-treatment TBR, which was defined as 100%, was calculated (relative TBR). FDG-PET analysis of control animals revealed a significant increase in FDG uptake on day 5 (n=4, mean 2.1-fold increase, SD=0.7, range 1.9-3.3-fold, p=0.03) (Fig. 2B). In AUY922 treated animals, relative TBR of early FDG-PET did not show a significant reduction

compared to the pre-treatment control (n=12, mean TBR 87%, SD=40.3%, range 31-161%; p=0.151). Interestingly, the mean TBR of FDG uptake at later time points (day 15 to 21) decreased to 44% (n=3, SD=33.6%, range 23-85%) (data not shown). In contrast to FDG assessment, the relative mean TBR of FLT uptake decreased significantly to 40% compared to baseline (n=12, SD=20.7%, range 32-67%, p=0.001) as early as 5 days after initiation of therapy (Fig. 2C). The relative TBR of untreated controls increased to more than 200% during the same time period (n=4, mean 2.1-fold increase, SD=0.6, range 1.6-3.0-fold p=0.01). Later time points within the treatment group (day 15 to 21) did not show any further reduction in FLT uptake (data not shown). To correlate the PET findings with the treatment effects of AUY922 on SUDHL-1 xenograft lymphomas, we stained fixed tumor sections for the proliferation marker Ki-67 and cleaved caspase-3 to analyze apoptosis. AUY922 treatment led to a significant increase in apoptosis as quantified by cleaved caspase-3 positive cells (Fig. 2D, n=5, mean 6.1%, SD=3.5%) compared to untreated mice (n=4, mean 1.6%, SD=1.1%; p=0.04). Moreover, the percentage of proliferating cells was substantially decreased by AUY922 as measured by Ki-67 staining with a mean of 15.3% (SD=0.8%) for the treated and 63.3% (SD=7%) for the control tumors (p=0.03). Taken together, both FDG as well as FLT uptake correlates with response to HSP90 inhibition *in vivo*. However, FLT-PET is highly superior to FDG-PET for early *in vivo* response assessment that precedes the change of tumor volume.

## Functional imaging of mTOR inhibition in ALCL xenografts by FLT-PET is superior to FDG-PET

To confirm the predictive value of FLT-PET imaging for early response evaluation using targeted agents, we treated mice bearing SUDHL-1 xenograft tumors with the mTOR inhibitor everolimus, and evaluated the efficacy of FDG- and FLT-PET monitoring. NPM-ALK-positive cells have previously been shown to undergo cell cycle arrest and apoptosis upon mTOR inhibition (27). Again, treatment was started when mice had measurable tumors. As depicted in Fig. 3A, tumor growth was completely inhibited by everolimus (mean 1.2-fold increase, SD=0.7, range 0.5-2.3 fold), whereas the size of control tumors steadily increased over time (mean 5.6-fold, SD=1.6). By using FDG-PET only a marginal, non-significant reduction of tracer uptake could be observed 5 days after therapy initiation compared to pre-treatment values (Fig. 3B). Although everolimus treated tumors revealed less FDG uptake compared to control tumors, this difference did not reach statistical significance. In contrast,

FLT-PET significantly discriminated between control and treatment group (Fig. 3C). We also found a modest, but statistically significant reduction of FLT uptake before and after initiation of everolimus application (p=0.01). Treated tumors harboured more cleaved caspase-3-positive cells compared to controls (Fig. 3D, 6.2% vs. 2.2%, p=0.04). Notably, exposure to everolimus dramatically decreased the percentage of Ki-67-positive cells from 57.1% to 20.3% (p<0.0001). Thus, functional imaging with FLT-PET rather than FDG-PET has a predictive value for response to mTOR inhibition.

These *in vivo* results were substantiated by further *in vitro* studies. Using MTT assays, we observed a reduction of cell growth to approximately 20% after incubation with 1nM everolimus for 48 hours compared to untreated cells (Supplementary Fig. S2A). At the same dose level, PI staining revealed a 50% decrease of cells in S phase and a marked increase of cells in G0/G1 phase (Fig. S2B), whereas the sub-G1 subset (Fig. S2B) and the AnnexinV-positive fraction (Fig. S2C) was low. *In vitro* efficacy could also be demonstrated by immunoblot analysis showing an abrogation of p70S6 kinase phosphorylation at a dose as low as 1nM (Suppl. Fig. S2D). In contrast to everolimus-responsive SUDHL-1 cells, other human ALCL cell lines that did not respond to everolimus treatment (defined as a reduction of S phase percentage or increase in apoptotic cells) showed no decrease in FLT uptake, again correctly predicting resistance. FDG-uptake correlated with cell cycle analysis and Annexin staining only in one cell line (Ba/F3-NA) (Fig. S3A-C).

### Validating the predictive value of FLT-PET imaging for therapy monitoring *in vivo*

To evaluate the selectivity of FLT-PET to predict response to targeted therapy, we used a different NPM-ALK expressing lymphoma cell line, Karpas299. Differently from SUDHL-1 ALCL cells, Karpas299 ALCL cells gave rise to xenograft tumors that were entirely resistant to targeted therapy with AUY922 (n=10, mean 3.2-fold increase, SD=0.4, range 2.9-3.6), resulting in a similar growth rate as control tumors (n=7, mean 5.2-fold increase, SD=1.5, range 2.8-7.6) (Fig. 4A). In contrast, everolimus treatment (n=8, mean 1.0-fold increase, SD=0.2, range 0.9-1.2) abrogated further Karpas299 tumor growth. FLT-PET scans were performed before and two days after initiation of therapy and relative TBRs of each treatment group were calculated. As expected, relative TBR of FLT uptake of both control and AUY922 treated animals did not differ from each other (p=0.42, Fig. 4B) and increased to a mean of 154% (range 107-202%; SD=35.5%) and 149% (range 46% to 175%, SD=47.2%),

respectively. Most importantly, FLT-PET imaging showed a significant decrease of the relative TBR of everolimus-treated Karpas299 tumors compared to the respective control (mean 92%, SD=37%, range 44-163%, p=0.001), again correctly predicting tumor growth kinetics. Thus, FLT-PET seems to be suitable to discriminate very early between response and resistance to targeted therapy. The PET findings were confirmed by immunohistochemistry. Compared to vehicle, everolimus induced a significant increase of apoptosis as detected by caspase-3 staining (Fig. 4C, mean=12.3%, SD=2.2% vs. mean=0.8%, SD=0.04%, p=0.02). In contrast, no significant induction of apoptosis was detected after AUY922 treatment compared to control tumors (mean=1.0%, SD=0.5%, p=0.5). In addition, the percentage of Ki-67 positive cells was significantly reduced after treatment with everolimus (Fig. 4D, mean=37.1%, SD=2.3%) in contrast to control tumors (mean=59.9%, SD=5.6%, p=0.02), indicating a strong induction of cell cycle arrest. AUY922 also led to a slight reduction of Ki-67 staining, however not to the level of statistical significance (mean=45.1%, SD=3.1%, p=0.1). Taken together, these data strongly support superiority of FLT-PET imaging for response prediction *in vivo*, thus allowing an early distinction between sensitive and refractory disease.

Since Karpas299 ALCL cells were not responsive to HSP90 inhibition by AUY922 treatment but sensitive to mTOR inhibition by everolimus *in vivo*, we assessed the effect of both drugs on Karpas299 cells *in vitro*. Karpas299 cells were exposed to escalating doses of AUY922. After a treatment period of 48hr cell cycle distribution was analyzed by PI staining. Fig. 5A shows that AUY922 had virtually no effect on cell cycle distribution. In accordance with the *in vivo* data, Karpas299 were sensitive to everolimus treatment resulting in an approximately 50% reduction of cells in S phase compared to control cells (Fig. 5A), while apoptosis was not increased (Fig. 5B). To evaluate the distinct biological effects of HSP90 and mTOR inhibition, we analyzed the biochemical effects by immunoblotting (Fig. 5C). Consistent with the PI staining and xenograft results and in sharp contrast to SUHDL-1 cells, HSP90 inhibition did not downregulate ALK phosphorylation or ALK protein levels. Moreover, the downstream targets phospho-Akt and Akt levels as well as phospho-STAT3 and STAT3 levels were virtually unchanged upon AUY922 treatment up to concentrations of 50nM and 100nM, respectively. Importantly, incubation of Karpas299 cells with everolimus abrogated the phosphorylation of the mTOR downstream target p70S6 kinase at the same dose level (1nM) compared to SUDHL-1 cells (Fig. 5C). These data indicate a strong concordance between early response evaluation by FLT-PET *in vivo*, tumor growth *in vivo*,

and effective *in vitro* pathway inhibition. Our studies thus provide strong evidence that FLT-PET appears to be highly suitable to predict early response to targeted therapy *in vivo*.

## Discussion

Ongoing progress in the understanding of lymphoma pathogenesis leads to the large-scale development of a multitude of pathway targeting drugs (30, 31). To optimize design and interpretation of clinical trials it will be crucial to identify biomarkers of sensitivity and response. These markers will also accelerate validation of effective drug combinations in the preclinical setting. Though pharmacodynamic biomarkers assess target inhibition and pathway downregulation, this does not necessarily equate with clinical benefit (32). In addition, many biomarker assays have been neither standardized nor validated (33). Thus, it is unlikely that in the majority of patients with advanced lymphoma the mere presence of a biomarker, a genetic profile, or an activated pathway will suffice to predict response to targeted therapy. Functional *in vivo* imaging could therefore be useful to assess and predict response to a specific treatment very early upon treatment initiation, at a time point, when conventional imaging cannot be expected to detect either response or resistance.

Our studies used the molecularly defined lymphoma entity ALCL, characterized by ALK-dependent pathway activation, to functionally evaluate the standard PET tracer FDG and the thymidine analogue FLT as early response markers. Constitutive ALK activation is a characteristic of NPM-ALK positive lymphoma and results in the activation of PI3K-AKT-mTOR and JAK-STAT signalling. Both are critical survival and proliferation pathways and have been proposed as pharmacologic targets for malignant diseases including lymphoma (24, 34, 35). Based on the defined oncogene and subsequently deregulated signal transduction, we felt that these lymphoma cells are most suitable for a translational approach comprising both *in vitro* and *in vivo* assays. HSP90 has been identified as an attractive target for anticancer therapy, since its inhibition effectively induced apoptosis in $ALK^+$ ALCL through the accelerated degradation of NPM-ALK and other proteins (26, 36). Everolimus is an approved mTOR inhibitor that has also shown efficacy in numerous tumors (37). We show that FLT uptake by lymphoma cells during inhibition of NPM-ALK or NPM-ALK downstream pathways closely reflected antiproliferative response. Moreover, there was a strong correlation between *in vivo* and *in vitro* results including western blot analyses assessing the activation of NPM-ALK and NPM-ALK-dependent pathways. Most importantly, early

changes of TBR of FLT-, but not FDG-PET, preceded change of tumor volume thus allowing distinction between sensitive and resistant cell lines and prediction of therapy response.

FDG-PET after completion of therapy is the non-invasive modality of choice for response classifications of aggressive lymphomas (5). Regarding interim FDG-PET during lymphoma treatment recent clinical studies investigating its predicitive value have clearly attenuated the validity in this scenario (10, 38). Moreover, FDG-PET did not predict tumor response during mTOR inhibition both in patients with advanced solid tumors and murine xenograft models (39) emphasizing the need for new surrogate markers reflecting early antiproliferative rather than metabolic response. FLT has been shown to accumulate in a variety of tumor entities due to intracellular trapping upon phosphorylation by the S phase enzyme thymidine kinase 1 (TK1) (13, 15, 16, 40). The correlation between TK1 activity and cellular uptake renders FLT an excellent surrogate marker of proliferation (14).

The lack of FDG to reflect tumor response early after initiation of HSP90 or mTOR-targeted therapy is in accordance with results from other preclinical models for breast (41, 42), ovarian (43) and pancreatic cancer (39). It is likely that an influx of inflammatory cells which can be observed already 48 hours after mTOR inhibition (44) contributes to higher FDG-uptake *in vivo*. Since FDG-uptake of inflammatory cells is similar or may even exceed that of tumor cells, transient increase in stromal reaction may result in overestimation of viable tumor (45). The observed dispersion of FDG uptake might also be attributed to a variable degree of inhibition of glycolysis as a consequence of disruption of the AKT-pathway resulting in altered FDG-uptake (39, 46). On the contrary, FLT uptake has been proven as a valid imaging biomarker for abrogation of the PI3K-AKT-mTOR pathway in solid tumors (43, 47). Inhibition of the NPM-ALK downstream pathway is known to induce cell-cycle arrest in G1 phase due to increase of p27 and decrease of cyclin D1 expression, a state resulting in low TK1 activity (48). Being a substrate of TK1, FLT thus appears as the ideal surrogate marker for inhibition of this pathway. Consistantly, we observed a significant reduction of FLT uptake on day 5 after commencement of both HSP90 and mTOR inhibition as measured by TBR of FLT-PET. Effective targeting was validated by documentation of tumor growth and immunostaining of explanted lymphomas, which revealed both a significant reduction of the proliferation and an increase of apoptosis.

Of note, we found a significant increase of apoptosis in lymphomas treated with everolimus *in vivo*, but not *in vitro*. This gives rise to the hypothesis that not only targets within the tumor cell, but also within the microenviroment of the tumor seem to contribute to tumor control. Indeed, everolimus potently inhibits growth of stromal and endothelial cells *in*

*vitro* and reduces tumor vascularization *in vivo* (49). However, PET monitoring of anti-angiogenic effects of everolimus failed both with FDG- and FLT-PET in several tumor entities (50). These observations as well as the fact, that inhibition of cell proliferation can be a transient phenomenon in the setting of intermittent drug administration (43, 44) underline the importance of careful consideration of pharmacodynamics in designing imaging protocols for response assessment.

Here we present a translational study including molecular, cellular, as well as *in vivo* analyses to validate the predictive value of PET for early assessment of response to targeted treatment. Our data provide strong evidence that FLT-, but not FDG-uptake represents a reliable, non-invasive surrogate marker to distinguish between sensitive and resistant lymphoma early after treatment initiation. These findings will facilitate rapid preclinical and clinical evaluation of novel inhibitors targeting this pathway.

## Acknowledgements

We thank Alexander Hildebrandt, Sabine Pirsig, Jolanta Slawska, Brigitte Dzewas and Coletta Kruschke for expert technical support. Supported by the Deutsche Forschungsgemeinschaft (SFB 824 and SFB TRR54).

## References

1. Michallet AS, Coiffier B. Recent developments in the treatment of aggressive non-Hodgkin lymphoma. Blood Reviews. 2009;23:11-23.
2. Dupire S, Coiffier B. Targeted treatment and new agents in diffuse large B cell lymphoma. Int J Hematol. 2010;92:12-24.
3. Younes A. Beyond chemotherapy: new agents for targeted treatment of lymphoma. Nature Reviews Clinical Oncology. 2011;8:85-96.
4. Cheson BD. Role of functional imaging in the management of lymphoma. J Clin Oncol. 2011;29:1844-54.
5. Juweid ME, Stroobants S, Hoekstra OS, Mottaghy FM, Dietlein M, Guermazi A, et al. Use of positron emission tomography for response assessment of lymphoma: consensus of the Imaging Subcommittee of International Harmonization Project in Lymphoma. J Clin Oncol. 2007;25:571-8.

6. Haioun C, Itti E, Rahmouni A, Brice P, Rain JD, Belhadj K, et al. [18F]fluoro-2-deoxy-D-glucose positron emission tomography (FDG-PET) in aggressive lymphoma: an early prognostic tool for predicting patient outcome. Blood. 2005;106:1376-81.
7. Mikhaeel NG, Hutchings M, Fields PA, O'Doherty MJ, Timothy AR. FDG-PET after two to three cycles of chemotherapy predicts progression-free and overall survival in high-grade non-Hodgkin lymphoma. Ann Oncol. 2005;16:1514-23.
8. Pregno P, Chiappella A, Bello M, Botto B, Ferrero S, Franceschetti S, et al. The interim 18-FDG-PET/CT failed to predict the outcome in diffuse large B-cell lymphoma patients treated at the diagnosis with rituximab-CHOP. Blood. 2012.
9. Moskowitz CH, Zelenetz A, Schoder H. An update on the role of interim restaging FDG-PET in patients with diffuse large B-cell lymphoma and Hodgkin lymphoma. J Natl Compr Canc Netw. 2010;8:347-52.
10. Moskowitz CH, Schoder H, Teruya-Feldstein J, Sima C, Iasonos A, Portlock CS, et al. Risk-Adapted Dose-Dense Immunochemotherapy Determined by Interim FDG-PET in Advanced-Stage Diffuse Large B-Cell Lymphoma. J Clin Oncol. 2010;28:1896-903.
11. Shreve PD, Anzai Y, Wahl RL. Pitfalls in oncologic diagnosis with FDG PET imaging: physiologic and benign variants. Radiographics. 1999;19:61.
12. Buck AC, Schirrmeister HH, Guhlmann CA, Diederichs CG, Shen C, Buchmann I, et al. Ki-67 immunostaining in pancreatic cancer and chronic active pancreatitis: does in vivo FDG uptake correlate with proliferative activity? Journal of Nuclear Medicine. 2001;42:721.
13. Shields AF, Grierson JR, Dohmen BM, Machulla HJ, Stayanoff JC, Lawhorn-Crews JM, et al. Imaging proliferation in vivo with [F-18] FLT and positron emission tomography. Nature medicine. 1998;4:1334-6.
14. Buck AK, Bommer M, Stilgenbauer S, Juweid M, Glatting G, Schirrmeister H, et al. Molecular imaging of proliferation in malignant lymphoma. Cancer research. 2006;66:11055.
15. Buck AK, Halter G, Schirrmeister H, Kotzerke J, Wurziger I, Glatting G, et al. Imaging proliferation in lung tumors with PET: 18F-FLT versus 18F-FDG. Journal of Nuclear Medicine. 2003;44:1426.
16. Kenny LM, Vigushin DM, Al-Nahhas A, Osman S, Luthra SK, Shousha S, et al. Quantification of cellular proliferation in tumor and normal tissues of patients with breast cancer by [18F] fluorothymidine-positron emission tomography imaging: evaluation of analytical methods. Cancer research. 2005;65:10104.
17. Wagner M, Seitz U, Buck A, Neumaier B, Schultheiß S, Bangerter M, et al. 3 -[18F] fluoro-3 -deoxythymidine ([18F]-FLT) as positron emission tomography tracer for imaging proliferation in a murine B-cell lymphoma model and in the human disease. Cancer research. 2003;63:2681.
18. Buck AK, Kratochwil C, Glatting G, Juweid M, Bommer M, Tepsic D, et al. Early assessment of therapy response in malignant lymphoma with the thymidine analogue [18 F] FLT. European Journal of Nuclear Medicine and Molecular Imaging. 2007;34:1775-82.
19. Dittmann H, Dohmen B, Kehlbach R, Bartusek G, Pritzkow M, Sarbia M, et al. Early changes in [18 F] FLT uptake after chemotherapy: an experimental study. European Journal of Nuclear Medicine and Molecular Imaging. 2002;29:1462-9.
20. Graf N, Herrmann K, den Hollander J, Fend F, Schuster T, Wester HJ, et al. Imaging proliferation to monitor early response of lymphoma to cytotoxic treatment. Molecular Imaging and Biology. 2008;10:349-55.
21. Herrmann K, Wieder HA, Buck AK, Schoffel M, Krause BJ, Fend F, et al. Early response assessment using 3 '-Deoxy-3 '-[F-18]fluorothymidine-positron emission tomography in high-grade non-Hodgkin's lymphoma. Clinical Cancer Research. 2007;13:3552-8.

22. Shiota M, Fujimoto J, Semba T, Satoh H, Yamamoto T, Mori S. Hyperphosphorylation of a novel 80 kDa protein-tyrosine kinase similar to Ltk in a human Ki-1 lymphoma cell line, AMS3. Oncogene. 1994;9:1567-74.
23. Morris SW, Kirstein MN, Valentine MB, Dittmer KG, Shapiro DN, Saltman DL, et al. Fusion of a Kinase Gene, Alk, to a Nucleolar Protein Gene, Npm, in Non-Hodgkins-Lymphoma. Science. 1994;263:1281-4.
24. Bai RYY, Tao OY, Miething C, Morris SW, Peschel C, Duyster J. NPM-ALK associated with anaplastic large-cell lymphoma activates the PI3-kinase/AKT antiapoptotic signaling pathway. Blood. 2000;96:469a-a.
25. Chiarle R, Simmons WJ, Cai HY, Dhall G, Zamo' A, Raz R, et al. Stat3 is required for ALK-mediated lymphomagenesis and provides a possible therapeutic target. Nature Medicine. 2005;11:623-9.
26. Bonvini P, Gastaldi T, Falini B, Rosolen A. Nucleophosmin-anaplastic lymphoma kinase (NPM-ALK), a novel hsp90-client tyrosine kinase: Down-regulation of NPM-ALK expression and tyrosine phosphorylation in ALK(+) CD30(+) lymphoma cells by the hsp90 antagonist 17-allylamino,17-demethoxygeldanamycin. Cancer Research. 2002;62:1559-66.
27. Vega F, Medeiros LJ, Leventaki V, Atwell C, Cho-Vega JH, Tian L, et al. Activation of mammalian target of rapamycin signaling pathway contributes to tumor cell survival in anaplastic lymphoma kinase-positive anaplastic large cell lymphoma. Cancer Research. 2006;66:6589-97.
28. Machulla HJ, Blocher A, Kuntzsch M, Piert M, Wei R, Grierson J. Simplified labeling approach for synthesizing 3 -deoxy-3 -[18F] fluorothymidine ([18F] FLT). Journal of Radioanalytical and Nuclear Chemistry. 2000;243:843-6.
29. Shiota M, Fujimoto J, Semba T, Satoh H, Yamamoto T, Mori S. Hyperphosphorylation of a Novel 80 Kda Protein-Tyrosine Kinase Similar to Ltk in a Human Ki-1 Lymphoma Cell-Line, Ams3. Oncogene. 1994;9:1567-74.
30. Sawas A, Diefenbach C, O'Connor OA. New therapeutic targets and drugs in non-Hodgkin's lymphoma. Curr Opin Hematol. 2011;18:280-7.
31. Sweetenham JW. Molecular signatures in the diagnosis and management of diffuse large B-cell lymphoma. Current Opinion in Hematology. 2011;18:288-92.
32. Tabernero J, Rojo F, Calvo E, Burris H, Judson I, Hazell K, et al. Dose- and schedule-dependent inhibition of the mammalian target of rapamycin pathway with everolimus: a phase I tumor pharmacodynamic study in patients with advanced solid tumors. J Clin Oncol. 2008;26:1603-10.
33. Markman B, Dienstmann R, Tabernero J. Targeting the PI3K/Akt/mTOR pathway--beyond rapalogs. Oncotarget. 2010;1:530-43.
34. Slupianek A, Nieborowska-Skorska M, Hoser G, Morrione A, Majewski M, Xue L, et al. Role of phosphatidylinositol 3-kinase-Akt pathway in nucleophosmin/anaplastic lymphoma kinase-mediated lymphomagenesis. Cancer research. 2001;61:2194.
35. Zamo A, Chiarle R, Piva R, Howes J, Fan Y, Chilosi M, et al. Anaplastic lymphoma kinase (ALK) activates Stat3 and protects hematopoietic cells from cell death. Oncogene. 2002;21:1038-47.
36. Kaiser M, Lamottke B, Mieth M, Jensen MR, Quadt C, Garcia Echeverria C, et al. Synergistic action of the novel HSP90 inhibitor NVP AUY922 with histone deacetylase inhibitors, melphalan, or doxorubicin in multiple myeloma. European journal of haematology. 2010;84:337-44.
37. Witzig TE, Reeder CB, LaPlant BR, Gupta M, Johnston PB, Micallef IN, et al. A phase II trial of the oral mTOR inhibitor everolimus in relapsed aggressive lymphoma. Leukemia. 2011;25:341-7.

38. Han HS, Escalon MP, Hsiao B, Serafini A, Lossos IS. High incidence of false-positive PET scans in patients with aggressive non-Hodgkin's lymphoma treated with rituximab-containing regimens. Ann Oncol. 2009;20:309-18.
39. Ma WW, Jacene H, Song D, Vilardell F, Messersmith WA, Laheru D, et al. [18F]fluorodeoxyglucose positron emission tomography correlates with Akt pathway activity but is not predictive of clinical outcome during mTOR inhibitor therapy. J Clin Oncol. 2009;27:2697-704.
40. Wagner M, Seitz U, Buck A, Neumaier B, Schultheiss S, Bangerter M, et al. 3'-[18F]fluoro-3'-deoxythymidine ([18F]-FLT) as positron emission tomography tracer for imaging proliferation in a murine B-Cell lymphoma model and in the human disease. Cancer Res. 2003;63:2681-7.
41. Smith-Jones PM, Solit D, Afroze F, Rosen N, Larson SM. Early tumor response to Hsp90 therapy using HER2 PET: comparison with 18F-FDG PET. Journal of Nuclear Medicine. 2006;47:793-6.
42. Bergstrom M, Monazzam A, Razifar P, Ide S, Josephsson R, Langstrom B. Modeling spheroid growth, PET tracer uptake, and treatment effects of the Hsp90 inhibitor NVP-AUY922. Journal of Nuclear Medicine. 2008;49:1204-10.
43. Jensen MM, Erichsen KD, Bjorkling F, Madsen J, Jensen PB, Hojgaard L, et al. Early detection of response to experimental chemotherapeutic Top216 with [18F]FLT and [18F]FDG PET in human ovary cancer xenografts in mice. PloS one. 2010;5:e12965.
44. Brepoels L, Stroobants S, Verhoef G, De Groot T, Mortelmans L, De Wolf-Peeters C. (18)F-FDG and (18)F-FLT uptake early after cyclophosphamide and mTOR inhibition in an experimental lymphoma model. Journal of Nuclear Medicine. 2009;50:1102-9.
45. Kubota R, Yamada S, Kubota K, Ishiwata K, Tamahashi N, Ido T. Intratumoral distribution of fluorine-18-fluorodeoxyglucose in vivo: high accumulation in macrophages and granulation tissues studied by microautoradiography. Journal of Nuclear Medicine. 1992;33:1972-80.
46. Plas DR, Thompson CB. Akt-dependent transformation: there is more to growth than just surviving. Oncogene. 2005;24:7435-42.
47. Fuereder T, Wanek T, Pflegerl P, Jaeger-Lansky A, Hoeflmayer D, Strommer S, et al. Gastric cancer growth control by BEZ235 in vivo does not correlate with PI3K/mTOR target inhibition but with [18F]FLT uptake. Clin Cancer Res. 2011;17:5322-32.
48. Manning BD, Cantley LC. AKT/PKB signaling: Navigating downstream. Cell. 2007;129:1261-74.
49. Lane HA, Wood JM, McSheehy PMJ, Allegrini PR, Boulay A, Brueggen J, et al. mTOR Inhibitor RAD001 (Everolimus) Has Antiangiogenic/Vascular Properties Distinct from a VEGFR Tyrosine Kinase Inhibitor. Clinical Cancer Research. 2009;15:1612-22.
50. Honer M, Ebenhan T, Allegrini PR, Ametamey SM, Becquet M, Cannet C, et al. Anti-Angiogenic/Vascular Effects of the mTOR Inhibitor Everolimus Are Not Detectable by FDG/FLT-PET. Translational Oncology. 2010;3:264-U172.

## Figure legends

**Figure 1.** FLT uptake is a sensitive measure for HSP90 inhibition of NPM-ALK+ ALCL *in vitro*. SUDHL-1 cells were treated with the indicated concentrations of AUY922 for 48hr. A,

cell viability was assessed by MTT assay. B, left panel, cell cycle distribution assessed by PI flow cytometry. The bars represent the mean±SD of the mean from n=3 individual experiments. B, right panel, apoptotic cell death upon AUY922 treatment assessed by flow cytometry for AnnexinV (AnnV) positivity. The bars represent the mean±SD of the mean, n=3. The upper part of the right panel figure shows representative histograms for each indicated treatment condition. C, assessment of phosphorylation and total protein levels upon target inhibition by immunoblotting. D, cellular tracer-uptake measurements were performed as described in the material and methods section 48hr after treatment with the indicated concentration of AUY922. Shown are the means±SD, n=3.

**Figure 2.** Functional *in vivo* monitoring of response to HSP90 inhibition in SUDHL-1 lymphoma by FLT-PET is superior to FDG-PET. Mice were treated with AUY922 (n=12 mice per group, 25mg/kg i.p. daily) or glucose 5% (n=4, i.p. daily) once tumors had reached a volume of approximately 500mm$^3$ (day 0). Some mice were sacrificed to explant lymphomas for immunohistochemical analysis (AUY922 group: n=5, day 5; control group: n=4, day 11-14). Remaining animals were monitored for tumor growth until day 14. A, tumor growth measurements. FDG- (B) and FLT-PET (C) scans were performed before (day 0) and 5 days after therapy initiation. Left panels, representative PET scans showing change of tumor tracer uptake (arrows). Right panels, TBR was calculated and served as an indicator of tracer uptake. TBR on day 0, defined as 100% ("pre"), and change of TBR compared to pre-treatment values are shown for treated ("post") and control animals. Mean TBR of FLT-PET (p=0.001) was significantly reduced in contrast to TBR of FDG-PET (p=0.15). D, immunohistochemistry of explanted lymphomas after 5 days of treatment using the apoptotis marker cleaved caspase-3 and the proliferation marker Ki-67. A-D, mean ±SD is shown.

**Figure 3.** Functional *in vivo* imaging of mTOR inhibition in SUDHL-1 ALCL xenografts by FLT-PET is superior to FDG-PET. Mice were treated with everolimus (n=12, 5mg/kg p.o. daily) or glucose 5% (n=7, p.o. daily) when xenotransplants reached a volume of approximately 500mm$^3$ (day 0). Some mice were sacrificed to explant lymphomas for immunohistochemical analysis (everolimus group: n=6, day 5; control group: n=4, day 11-14) and remaining animals were monitored for tumor growth until day 14. A, tumor growth in everolimus-treated and control mice. FDG- (B) and FLT-PET (C) was performed before (day 0) and 5 days after therapy initiation. Left panels: representative PET scans showing change of tumor tracer uptake (arrows). Right panels: TBR was calculated and served as an indicator

of tracer uptake. TBR on day 0, defined as 100% ("pre"), and change of TBR compared to pre-treatment values are shown for treated ("post") and control animals. Mean TBR of FLT-PET was significantly reduced in contrast to TBR of FDG-PET. D, immunohistochemistry of explanted lymphomas using the apoptosis marker cleaved caspase-3 and the proliferation marker Ki-67. A-D, mean ±SD is shown.

**Figure 4.** FLT-PET imaging for response prediction *in vivo* allows the early distinction between sensitive and refractory disease. Mice were treated with everolimus (n=8, 5mg/kg p.o. daily), AUY922 (n=10, 25mg/kg i.p. daily) or glucose 5% (n=7, p.o. daily) when Karpas299 xenotransplants reached a volume of approximately 500mm$^3$ (day 0). Some mice were sacrificed (day2) to explant lymphomas for immunohistochemistry (everolimus group: n=3; AUY922 group: n=3; control group: n=3) and remaining animals were monitored for tumor growth until day 8. A, tumor growth. B, FLT-PET was performed before (day 0) and two days after therapy initiation. Left panel: TBR was calculated and served as an indicator of tracer uptake. TBR on day 0 was defined as 100%. Change of TBR compared to pre-treatment value is shown for each group. Right panel: representative PET scans showing change of tumoral tracer uptake (arrows). C, immunohistochemistry of explanted lymphomas upon treatment with the indicated drugs using the apoptotis marker cleaved caspase-3. D, analysis of proliferation by Ki-67 immunohistochemistry. A-D, mean±SD is shown.

**Figure 5.** Concordance between cell cycle state and pathway inhibition. Karpas299 cells were cultured with AUY922 or everolimus as indicated for 48hr. A, cell cycle distribution assessed by PI flow cytometry. The upper panels show representative DNA histograms, the lower panels show quantification from n=3 experiments. The bars represent the mean±SD. B, assessment of apoptosis by AnnexinV (AnnV) flow cytometry. The upper panels show representative dot blot analyses, the lower panels show the mean±SD (n=3). C, validation of target inhibition by immunoblotting was performed using the indicated antibodies. Cell cycle distribution and NPM-ALK signalling was not affected by AUY922 (A, left; C, left). In contrast, everolimus induced G1 arrest with consecutive reduction of cells entering S phase (A, right panels). In addition, phosphorylation of the mTOR downstream target protein p70S6 kinase (p70S6K) was completely abrogated at concentrations as low as 1nM (C, right).

Author Manuscript Published OnlineFirst on August 8, 2012; DOI:10.1158/0008-5472.CAN-12-0635
Author manuscripts have been peer reviewed and accepted for publication but have not yet been edited.

**Figure 1**

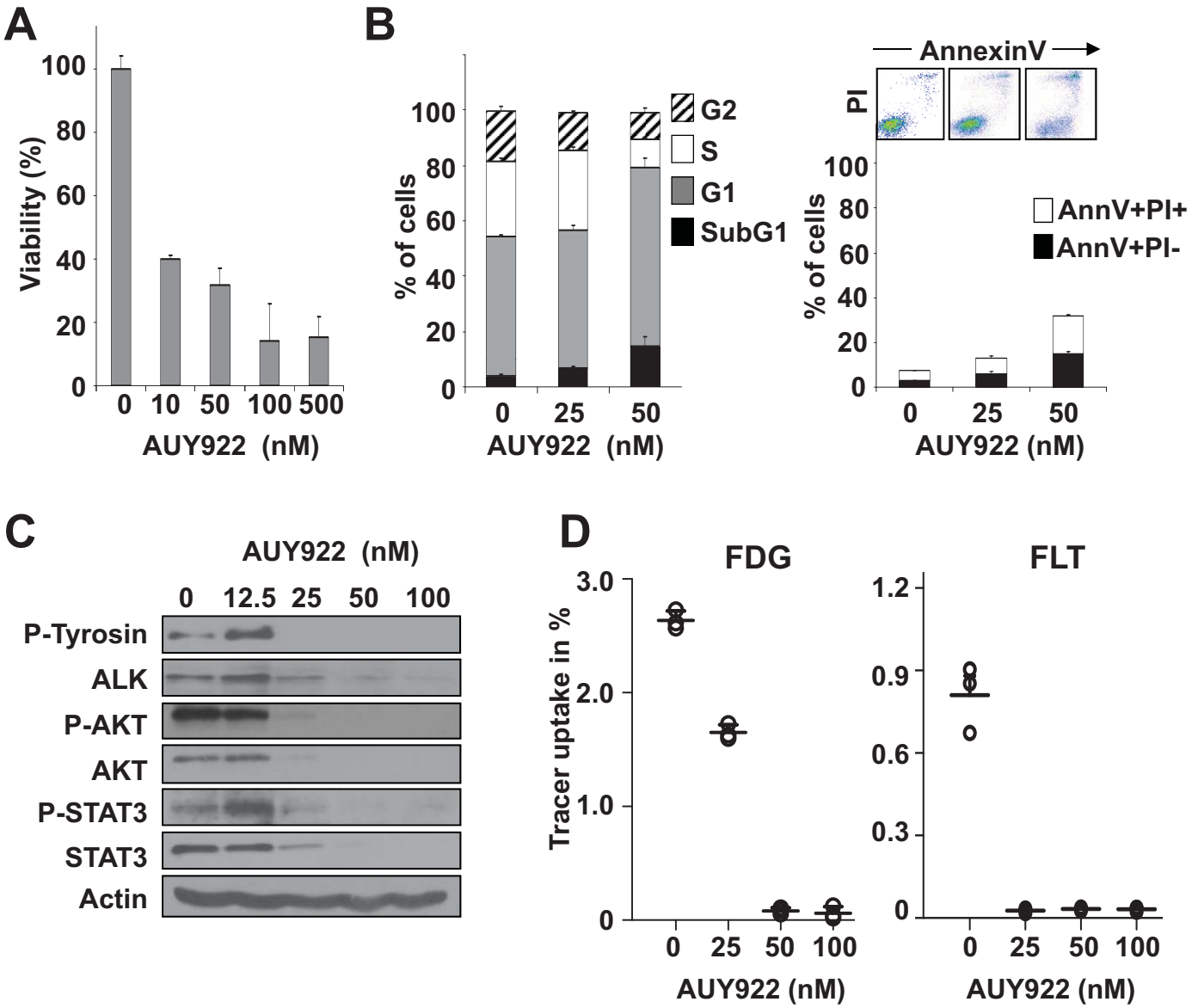

Author Manuscript Published OnlineFirst on August 8, 2012; DOI:10.1158/0008-5472.CAN-12-0635
Author manuscripts have been peer reviewed and accepted for publication but have not yet been edited.

Figure 2

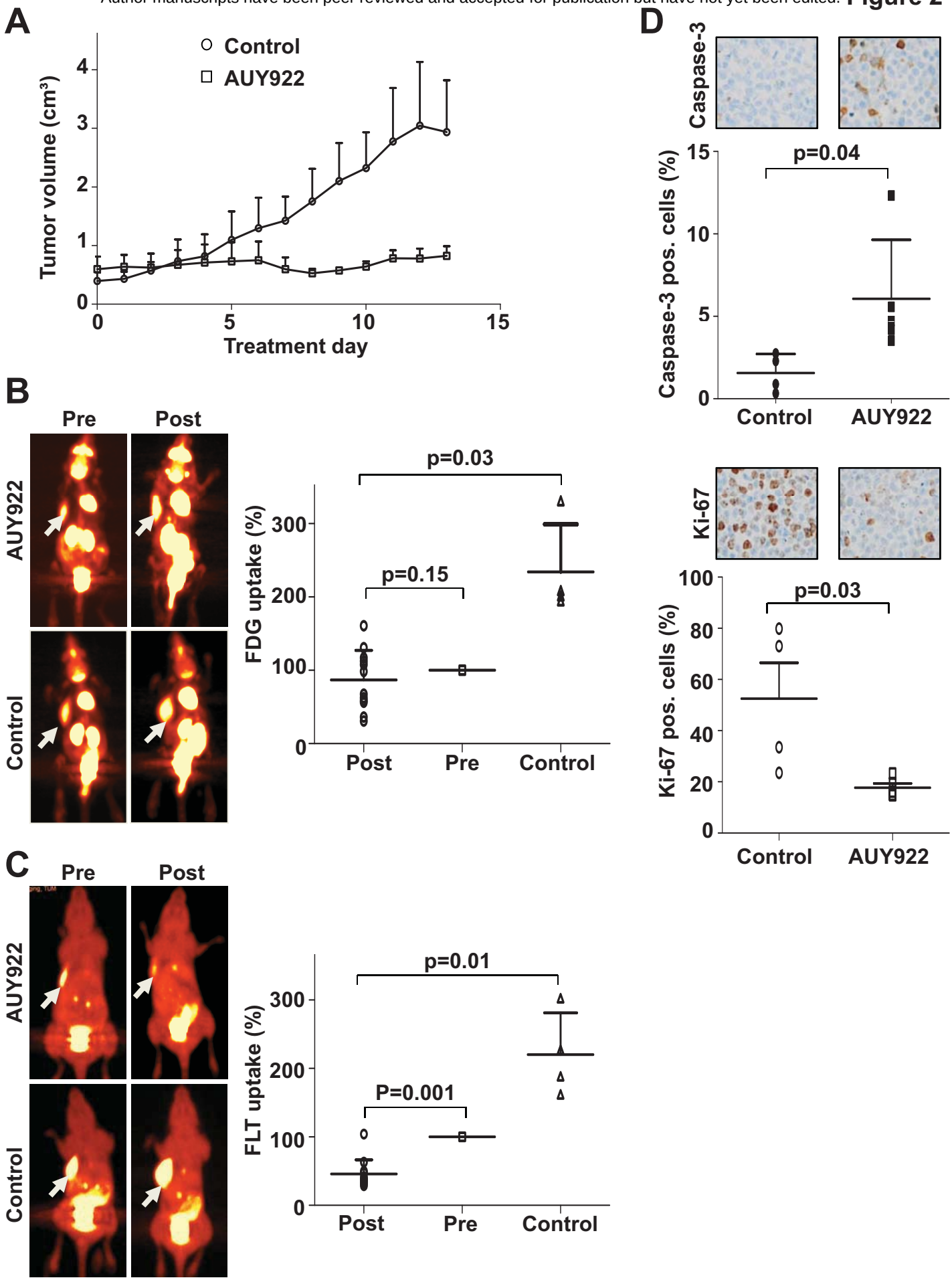

Author Manuscript Published OnlineFirst on August 8, 2012; DOI:10.1158/0008-5472.CAN-12-0635
Author manuscripts have been peer reviewed and accepted for publication but have not yet been edited.

**Figure 3**

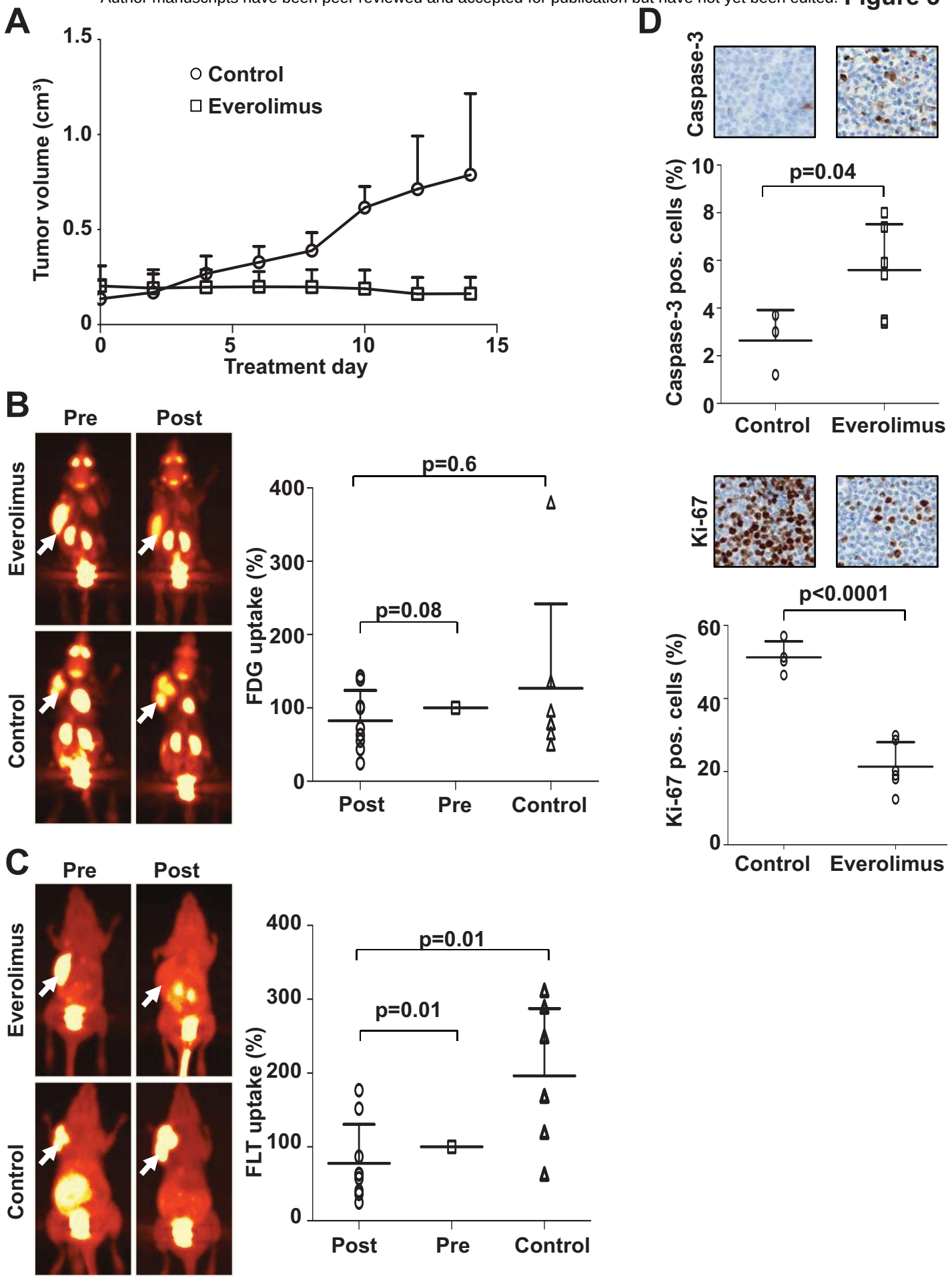

Author Manuscript Published OnlineFirst on August 8, 2012; DOI:10.1158/0008-5472.CAN-12-0635
Author manuscripts have been peer reviewed and accepted for publication but have not yet been edited.

**Figure 4**

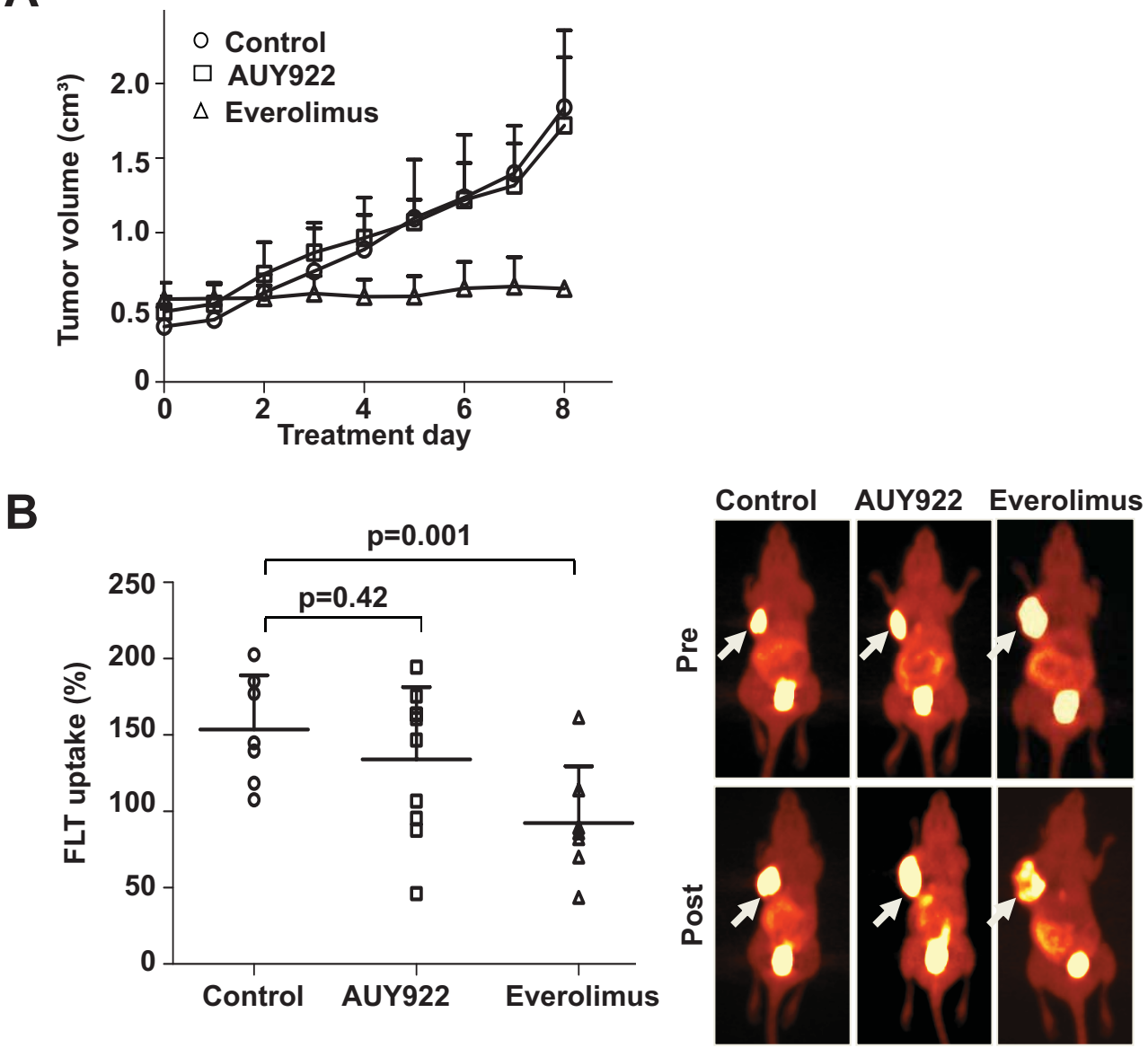

Author Manuscript Published OnlineFirst on August 8, 2012; DOI:10.1158/0008-5472.CAN-12-0635
Author manuscripts have been peer reviewed and accepted for publication but have not yet been edited.

**Figure 5**